ACS APPLIED MATERIALS & INTERFACES

Research Article

www.acsami.org

Adsorption and Diffusion of Li on Pristine and Defective Graphene

Xiaofeng Fan,*,† W.T. Zheng,*,† and Jer-Lai Kuo‡

†College of Materials Science and Engineering and Key Laboratory of Automobile Materials of MOE, Jilin University, Changchun 130012, China

‡Institute of Atomic and Molecular Sciences, Academia Sinica, Taipei, 10617, Taiwan

ABSTRACT: With first-principles DFT calculations, the interaction between Li and carbon in graphene-based nanostructures is investigated as Li is adsorbed on graphene. It is found that the Li/C ratio of less than 1/6 for the single-layer graphene is favorable energetically, which can explain what has been observed in Raman spectrum reported recently. In addition, it is also found that the pristine graphene cannot enhance the diffusion energetics of Li ion. However, the presence of vacancy defects can increase the ratio of Li/C largely. With double-vacancy and higher-order defects, Li ion can diffuse freely in the direction perpendicular to the graphene sheets and hence boost the diffusion energetics to some extent.

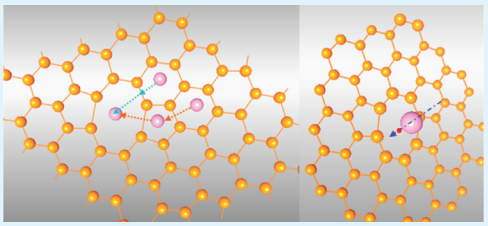

KEYWORDS: *first-principles calculations, graphene, rechargeable Li batteries, diffusion of Li, adsorption of Li, defects and nanostructures*

1. INTRODUCTION

Graphene has attracted enormous attention due to its fascinating physical properties,[1−3] such as ballistic electronic transport,[4] abnormal quantum Hall effects,[5] and massless Dirac fermions,[6] since it was found in 2004.[7] Being a stable single sheet of carbon atoms with honeycomb lattice, graphene also shows considerable promise as atom/molecule containers for the potential application on electrochemical storage devices,[8−10] such as rechargeable Li batteries (RLBs),[9] since both sides of it can hold the adsorbent and its edges can interact with other molecules.[11]

In most RLBs, graphite is used as anode instead of metallic Li electrode, considering both safety and cycle efficiency.[12] Comparing with the capacity (3860 mA h/g) of metallic Li, the biggest disadvantage of graphite is its low capacity (372 mA h/g).[13] As an intercalation compound, Li ion can be intercalated into the layers of graphite with the formation of stage-1.[14] However, every six carbon atoms just hold one Li atom for each layer to form LiC_6.[15] If one can boost the Li/C ratio, the performance of RLBs should be enhanced obviously. Carbonaceous nanostructures, such as carbon nanotubes[16−18] and graphene-based materials,[9] are considered to have extra storage sites and expected to make a large specific capacity.[11,19]

Graphene nanosheets are demonstrated experimentally to have a good cyclic performance and a specific capacity of 460 mA h/g after 100 cycles.[20] Disordered graphene nanosheets are found to have high reversible capacities in the range of 794−1054 mA h/g.[21] Oxidized graphene nanoribbons are reported to present an initial charge capacity of ∼1400 mA h/g with a reversible capacity of about 800 mA h/g.[22] These experimental results indicate that it is possible to increase the Li/C ratio to about 1/2. However, recent Raman spectrum on single-layer and few-layer graphene shows that the intercalation of Li in few-layer graphene resembles the case of graphite and the amount of Li adsorbed on single-layer graphene is reduced.[23] Theoretical investigation should help to deeply understand the different experimental phenomena and the nature of Li−C interaction.[24−28] The calculations of Khantha et al. show that Li can be adsorbed on graphene plane with a binding energy of 0.934−1.598 eV.[29] Chan et al. demonstrate that different adsorption positions have different adsorption energies.[30] The adsorption energies of hollow, bridge and top sites of graphene are 1.096, 0.773, and 0.754 eV, respectively.[30] Recently, Yang's calculation shows that Li_2C_2 with a binding energy of 1.40 eV is possible to be formed, like the case of graphane by hydrogenation.[31] This means that the theoretical value of Li/C ratio can be 1. Furthermore, the Li−C bond is considered to have a significant ionic character[32,33] which can make the diffusion of Li easier on graphene. Though a considerable effort toward the increase of Li/C ratio has been taken, the exact mechanism of intercalation/deintercalation of Li and Li−C interaction in these carbonaceous nanostructures are still not clear.[34]

In this work, using first-principle calculations, we try to make some light about Li−C interaction based on the theoretical models of Li adsorbed on pristine and defective graphene. Through our calculations, we confirm the previous conclusion that Li atoms can be adsorbed on the top sites of graphene from both sides with a large binding energy, which means a possibility of the formation of Li_2C_2. However, it should not be easy to synthesize Li_2C_2 experimentally, because Li atom is easier to be adsorbed on the hollow site with a very low concentration and large binding energy of about 1.3 eV/Li. Moreover, with the increase in Li concentration on graphene,

Received: January 18, 2012
Accepted: April 26, 2012
Published: April 26, 2012

the additional Li atom is more likely to stick on the Li ion, which has been adsorbed on graphene and is not directly adsorbed on the other unoccupied sites when the Li/C ratio is more than 1/6 for the single-layer graphene. Our simulations about the intercalation of Li in 2-layer graphene and 3-layer graphene confirm that the stage-1 compound LiC_6 can be formed for graphite. These results can explain the Raman spectroscopy experiments that the amount of Li adsorbed on single-layer graphene seems to be limited. We also study the diffusion of Li on graphene with a single layer and in between two layers for the bilayer graphene. Considering the presence of vacancy in graphene, we analyze the effects of single-vacancy and double-vacancy on the adsorption and diffusion of Li on graphene. It is found that Li ion can diffuse from one side to another side of graphene by double-vacancy. In addition, a potential trap is introduced around the vacancy, and this trap may increase the amount of Li ion adsorbed on graphene. With the analysis of charge distribution and electronic properties, the mechanism of interaction between Li and defective graphene is revealed.

2. THEORETICAL DETAILS

In this work, all the calculations have been carried out by employing the method of projector augmented wave potentials[35] based on density functional theory[36] as implemented in the VASP code.[37,38] The generalized gradient approximation (GGA) with the parametrization of Perdew–Burke–Ernzerhof (PBE)[39] is used to express the exchange-correlation energy of interacting electrons. The *k*-space integral and the plane-wave basis are chosen to ensure that the total energy is converged at the 1 meV/atom level. The kinetic energy cutoff of 550 eV for the plane wave expansion is found to be sufficient. The Monkhorst–Pack method is used to sample the k points in the Brillouin zone. Considered the magnetism of isolated Li atom and the possible magnetism of defective graphene, the spin-polarized calculation is also taken.

For the primitive unit cell of graphene, the two C atoms are placed on two-dimensional honeycomb lattice with a hexagonal structure. The lattice constant is chosen to be 2.464 Å, which is from the calculation of the lattice constant of graphite and is slightly larger than the experimental value 2.46 Å. Based on the primitive cell, different supercells including 2 × 2, 3 × 3, 4 × 4, and 6 × 6 hexagonal structures as the ideal models are used to analyze the Li adsorption. The Brillouin zones of 2 × 2, 3 × 3, 4 × 4, and 6 × 6 supercell are sampled with the Γ-centered k-point grid of 20 × 20 × 1, 16 × 16 × 1, 12 × 12 × 1, and 8 × 8 × 1, respectively. To avoid the spurious coupling effect of between graphene layers along *z*-axis when Li atom is adsorbed on graphene, the vacuum separation in the model structures is set to 18 Å. Due to the building of repeated supercell, the dipole corrections for potential and total energy are also considered. The use of 4 × 4 supercell can be used to simulate properly the interaction between an isolated Li and graphene with the small amount of calculation. This setup, which means the Li/C ratio of 1/32, corresponds to the in-plane constant of 9.86 Å which is also the distance between neighboring Li atoms. Therefore, the single-vacancy and double-vacancy are constructed in 4 × 4 supercell. The structures are relaxed with the modulation of lattice parameter and the positions of atoms are optimized fully. The change of lattice constants is found to be very small and can be ignored.

3. RESULTS AND DISCUSSION

3.1. Adsorption and Diffusion of Li on Pristine Graphene. To analyze the adsorption of Li on graphene, we consider three sites with high symmetry: the site on the top of a carbon atom (Top), the site at the midpoint of a carbon–carbon bond (Bridge), and the site in the center of a hexagon (Hex.). The adsorption energy is defined as

$$E_{ab} = (E_{ad-g} - nE_{ad} - E_g)/n$$

where $E_{ad\text{-}g}$ is the total energy of the compound in which Li is adsorbed on graphene, E_{ad} is that of an isolated Li atom, E_g is that of the isolated graphene of $n \times n$ supercell whose size corresponds to that of the Li-adsorbed graphene, and n is the number of adsorbed Li atoms. The geometry structure and adsorption energy are obtained after the positions of all the atoms have been relaxed. For the compound with a high Li concentration, such as Li_2C_2, it may occur that the sp^2 lattice of graphene is distorted and the lattice constant a is reduced due to the interaction between Li and C. Therefore, the relaxation of lattice constant a is also considered.

For Li_2C_2, the stablest configuration is that two Li atoms are adsorbed on top sites from both sides of graphene with a lattice constant of 2.586 Å, as shown in Figure 2E. The distance between carbon atoms and that between Li and C are 1.535 Å and 2.006 Å, respectively, which is similar to the recent calculations.[31] Though the carbon lattice of Li_2C_2 is crumpled due to the adsorption of Li atom, the lattice constant becomes larger than that (2.464 Å) of pure graphene, which can be attributed to the lengthening of C–C bond. The angles of C–C–C and C–C–Li are 114.8 and 76.7°, respectively. By comparing with the purely sp^2-bonding system, the C–C bond may be hypothesized to be a mixture of sp^3 and sp^2 bonding for the stable configuration of Li_2C_2, as mentioned by Klintenberg et al.[33] However, as the long Li–C bond should be different from the short H–C bond of graphane, Li–C bond should have a significant ionic character from the analysis of charge transfer (which will be mentioned in the next part) and the local distribution of electrons.[40] It is also worth noticing that the binding energy reported in ref 31 (1.40 eV) is larger than that (1.085 eV) of ref 32, whereas if the effect of spin-polarization for isolated Li atom is considered, our calculated result is 1.101 eV, which is similar to that from refs 30 and 32. However, if the effect of spin-polarization is not considered, our calculated binding energy is 1.34 eV. As the binding energy of 1.101 eV for Li_2C_2 is smaller than that (1.134 eV) of Li adsorbed on graphene with hexagon site (using the model of 4 × 4 supercell), whether Li_2C_2 is the stablest compound of Li–C still needs to be explored carefully. In additional, the long-range van der Waals forces should be considered due to the large polarization of Li atom.[41,42] On the basis of the analysis of Allouche et al.,[41] the absolute value of absorption energy of Li on graphene needs the energy correction of about 0.45 eV for the long-range dispersion contribution.

Figure 1 shows the adsorption energy of Li adsorbed on graphene as a function of Li concentration. It can be found that the adsorption on the hexagon site is more stable than the top site generally, as Li concentration varies from 0 to 50%. Especially, the adsorption on the hexagon site is most stable at the low Li concentration, such as LiC_{72}. As the Li concentration increases, the binding energy of Li adsorbed on hexagon site reduces. This can be attributed to the coulomb repulsion among Li ions on graphene as the electron transfers from Li to

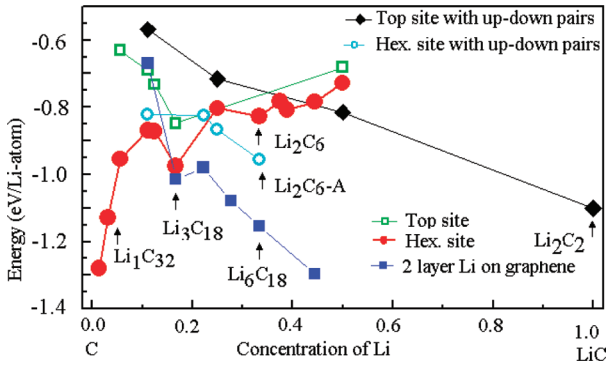

Figure 1. Adsorption energy as a function of Li concentration on graphene for different models, including the adsorption on top site, hexagon site, adsorption from both surface and two-layer Li adsorbed on graphene. Note that the structures of different concentrations calculated are with the unit cell 6 × 6, 4 × 4, 3 × 3, 2 × 2, and 1 × 1, respectively.

graphene, upon the adsorption of Li on graphene. For the up−down Li pairs adsorbed on the top site which is a bifacial adsorption, the binding energy decreases with decreasing Li concentration, which can be described to the effect of strain. Though the interaction between Li and C can make the sp^3−sp^2 hybridized stable for Li adsorbed graphene, the strain of sp^2 bonds near the special carbon atom will compensate the increase in binding energy upon the decrease in Li concentration. At the concentration of about 44%, the adsorption energy is similar to that of Li adsorption with hexagon site. Since the graphene has both surface and the adsorption on the hexagon site is the stablest for the low Li concentration, the adsorption of hexagon site with up−down pairs is also explored. Truly, the up−down configuration Li_2C_6-A (Figure 2B) is more stable than Li_2C_6 (Figure 2D) at the Li concentration of 33%, as shown in Figure 1. It is also found that the LiC_6 (Figure 2C) is a metastable phase in the curve of the adsorption energy on hexagon site vs Li concentration. This may help to explain why it is easy to form the stage-1 compound LiC_6 for graphite. However, the difference of adsorption energy between Li_2C_6-A and LiC_6 is just about 20 meV, and hence it seems that the Li concentration can be boosted from 16.7% to 33%, and even to 100% for the formation of Li_2C_2. This means a single-layer graphene may increase the Li/C ratio significantly upon the adsorption of Li on graphene.

From the adsorption energy curve for Li adsorbed on the hexagon site, it seems that the repulsion among Li ions results in elevating some Li ions from the plane of Li ions on graphene as Li concentration is increased. We have considered the configurations that have two layer Li atom adsorbed on graphene. As Li concentration is more than 1/6 (forming Li_3C_{18} in Figure 2), it is actually found that the configurations with bilayer Li are more stable. It means that the amount of Li adsorbed on single-layer graphene is not greater than that on graphite, which is consistent with the Raman spectrum results. Therefore, though Li_2C_2 is energetically stable, it will be difficult to obtain experimentally, because it will have the trend to congregate Li to form multilayer Li on graphene when the Li concentration is more than 16.7%. It is also noticed that the concentration of adsorbed Li in the region near the zigzag edge of graphene may be increased properly because of the edge effects.[43,44]

Lithium diffusion in carbonaceous nanostructures is still not understood fully because of the lack of reliable experimental methods.[45] This makes the theoretical evaluation of the diffusion barrier and path of Li ion important.[46] As shown in Figure 3A, two high symmetrical paths of Li diffusion on graphene (including (A) Hex.-Bridge-Hex. and (B) Hex.-Top-Hex.) are explored. For path A, the highest point of barrier is at bridge site with a energy of 0.311 eV and path length of 2.462 Å. For path B, the barrier is 0.337 eV at top site with a path length of 2.844 Å. Therefore, there are six paths with a lower barrier for Li diffusion on graphene. To analyze the diffusion in

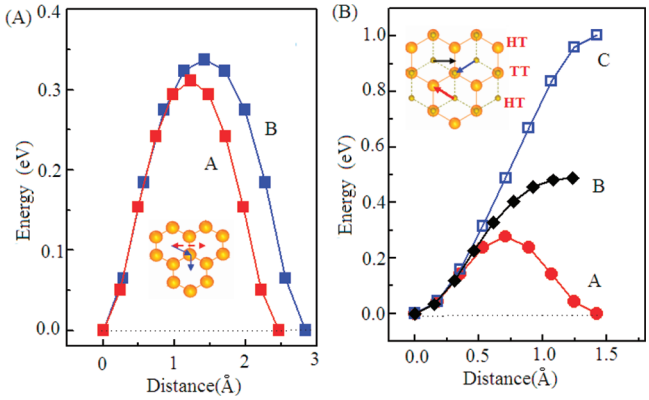

Figure 3. Potential-energy curves of (A) Li adsorbed graphene following two paths (Hex.-Bridge-Hex. and Hex.-Top-Hex.) shown by red and blue square-lines and (B) Li adsorbed in between two layers of graphene following three paths, including HT-HT (path A), HT-Bridge and HT-TT (path C), shown by red circle-line, black diamond-line and blue square-line.

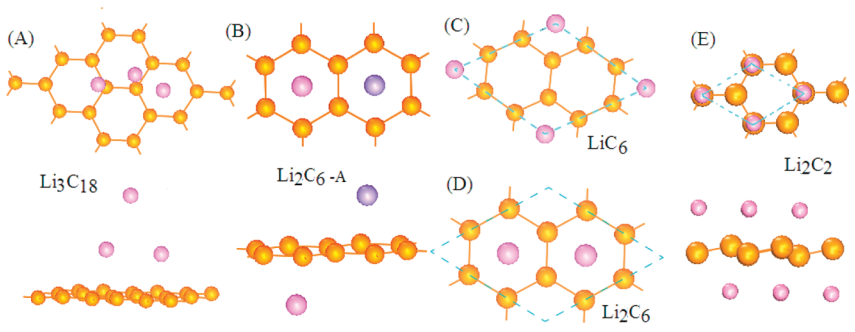

Figure 2. (A) Schematic representation of Li_3C_{18} for two-layer Li adsorbed graphene, (B) Li_2C_6-A for the Li adsorption on both surfaces, (C) LiC_6, (D) Li_2C_6 for the adsorption on hexagon site, and (E) Li_2C_2.

dx.doi.org/10.1021/am3000962 | ACS Appl. Mater. Interfaces 2012, 4, 2432−2438

between layers of graphite, we simulate the diffusion of Li in between two layers for bilayer graphene, and the distance between two layers is fixed and equal to half of lattice constant c of graphite. For the stage 1 compound LiC_6 of graphite, the adsorption on HT site (in Figure 3B) is the most stable. Three high symmetrical paths of Li diffusion on graphene are considered, including HT-HT (path A), HT-Bridge, and HT-TT (path C). As shown in Figure 3B, the path A has the lowest barrier (0.277 eV) with the path length of 1.421 Å. There are three paths with the lowest barrier for Li diffusion in between layers. Therefore, Li ion in between two layers of graphite diffuses more quickly than that on the surface of graphene, and the surface of pristine graphene can not boost the diffusion energetics of Li ion. Moreover, the diffusion coefficient is found to be reduced near the edge of graphene.[47] Therefore, the edge effects can boost the diffusion of Li in nanosized graphene to some extent.

3.2. Adsorption and Diffusion of Li on Defective Graphene. Intuitively, it should be difficult for Li ions to diffuse from one side of graphene to the other side. To probe the diffusion energetics of Li ion in the direction perpendicular to the graphene sheet, we considered three models, including pristine graphene, defective graphene with single-vacancy and that with double-vacancy, as shown in Figure 4A–C,

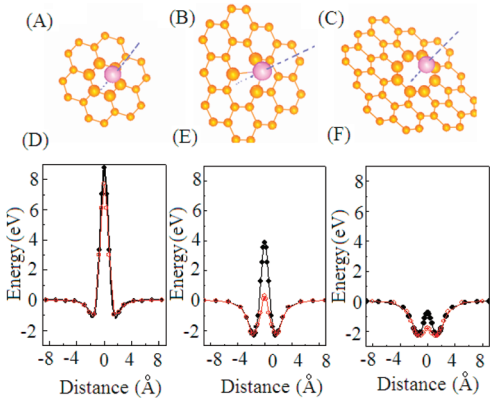

Figure 4. Schematic representations and potential-energy curves of Li diffusion in the direction perpendicular to the graphene sheet for (A, D) pristine graphene, (B, E) graphene with single-vacancy, and (C, F) graphene with double-vacancy.

respectively. For all three models, the pathway is characterized by the two local symmetrical minima and one maximum for the diffusion barrier. For the pristine graphene, the barrier energy is about 9.8 eV, and the local minimum is about 0.94 eV, located about 1.7 Å away from each side of graphene. When a Li ion is stuck at the position of the barrier, the lattice relaxes and the barrier energy is found to be reduced to 8.74 eV. Obviously, a large diffusion barrier makes it virtually impossible for Li ion to diffuse along the direction perpendicular to graphene. As show in Figure 4E, F and Table 1, the defect in graphene, especially the double-vacancy, significantly reduces the diffusion barrier of Li ion. It is clear that for the double-vacancy and higher-order defects, Li ion can freely diffuse from one side to the other side of the graphene plane. This result gives a support that the vacancy defects in graphene-based nanostructures can enhance the diffusion energetics of Li ion to some extent.

Because the defects are important for the Li diffusion energetics in graphene-based material. The diffusion of Li near the defects is also worthy exploring. As shown in Figure 5, two

Table 1. Diffusion Barrier ΔE, Diffusion Barrier $\Delta E'$ after Lattice Relaxation, Local Minimum ΔE_1, and the Position of Local Minima H for the Three Cases Shown in Figure 4

	ΔE (eV)	$\Delta E'$ (eV)	ΔE_1 (eV)	H (Å)
pristine graphene	9.80	8.74	0.94	1.7
single vacancy	6.22	2.59	2.28	1.6
double vacancy	1.55	0.54	2.30	1.4

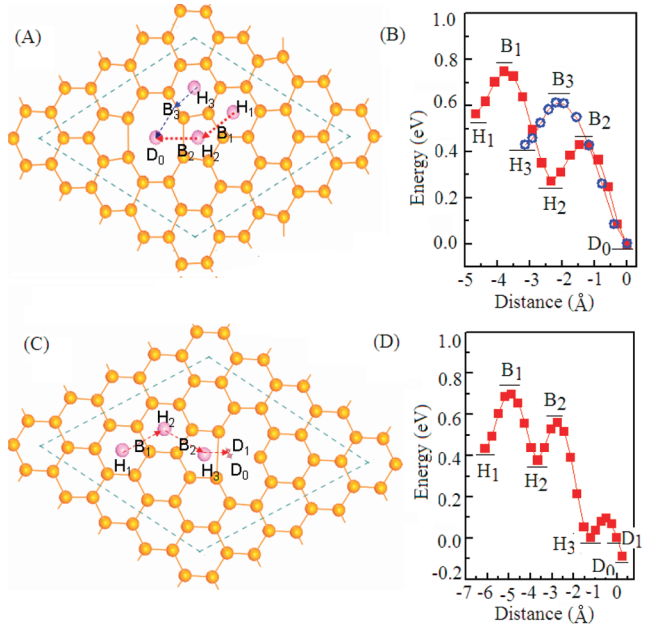

Figure 5. Schematic representations and potential-energy curves of (A, B) Li diffusion on graphene with double-vacancy following two paths (H_3–B_3–D_0 and H_1–B_1–H_2–B_2–D_0) shown in blue line and red line, and (C, D) diffusion on graphene with single-vacancy following the path H_1–B_1–H_2–B_2–H_3–D_1–D_0.

pathways for graphene with double-vacancy (H_3–B_3–D_0 and H_1–B_1–H_2–B_2–D_0) and one long pathway for graphene with single-vacancy (H_1–B_1-H_2–B_2-H_3-D_1-D_0) are analyzed. From Figure 5 B and D, it can find that the defect results in the formation of one potential trap around itself. For double-vacancy, the distance between H_1 and D_0 is about 4.6 Å and the energy difference is about 0.56 eV. For single-vacancy, the distance between H_1 and D_0 is about 6.1 Å and the energy difference is about 0.52 eV. The extra trap can enhance the adsorption energy and hence increase the Li/C ratio. Furthermore, the diffusion barrier between hexagon sites around the defect is about 0.17 eV for double-vacancy, and 0.24 eV for single-vacancy, which is even less than that of pristine graphene (0.311 eV). Therefore, the trap will not obviously reduce the diffusion energetics of Li ion on the surface of graphene. In addition, Li ion can diffuse easily to the vacancy and then go through the vacancy to another surface or the surface of other graphene layer for graphene-based nanostructures.

3.3. Electronic Properties of Graphene and Defective Graphene with Li-Adsorption. To analyze the nature of Li–graphene interaction, we compute the electronic structure of graphene with the adsorbed Li. In Figure 6, the band structure and density of states of graphene (DOS) with one adsorbed Li on hexagon site in 3 × 3 supercell are shown. Band structures are represented by k points along the three directions of symmetry in the irreducible Brillouin zone. Comparing with

dx.doi.org/10.1021/am3000962 | ACS Appl. Mater. Interfaces 2012, 4, 2432–2438

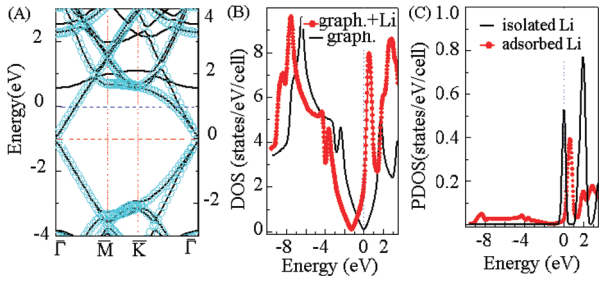

Figure 6. (A) Band structures and (B) density of states (DOS) of pristine graphene and Li-adsorbed graphene with 3 × 3 unit cell and (C) the partial density of states (PDOS) of isolated Li and adsorbed Li. Note that the DOS of isolated Li is the sum of spin-up bands and spin-down bands.

that of pristine graphene, the Li adsorption does not distinctly change the band structure of graphene, except the upshift of Fermi level. In addition, there is an extra energy band at about 1 eV above Fermi level upon the adsorption of Li on graphene. By comparing the PDOS of Li-adsorbed graphene with that of graphene, it is found that the extra energy band should be from Li 2s levels. From DOS of Li-adsorbed graphene and PDOS of the Li ion, it can find that the Li 2s peak is only partially occupied in the Li-graphene system. Therefore, the C−C bonds near the adsorbed Li ion should retain their sp^2 character and C atoms do not significantly rehybridize with any orbitals of Li atom. This supports that the interaction between Li and graphene is governed by charge transfer and the ionic bond is formed. In order to analyze the charge transfer quantitatively, the shift of Fermi level (ΔE_F) is calculated for the Li-adsorbed graphene with 4 × 4 supercell. The charge transfer (ΔQ_{DOS}) can be obtained by the integral of the DOS of free graphene from the energy of Dirac point (E_D) to the energy of $E_D + \Delta E_F$.[30] $\Delta Q_{DOS} \approx 0.94e$ is obtained from $\Delta E_F = 0.947$ eV for the lithium atomic concentration of 3.125%. The charge transfer can also be gained from the distribution of charge density. We can define the charge density difference by the formula[48] $\Delta\rho_{cd}(r) = \rho_{Li-g}(r) - \rho_{Li}(r) - \rho_g(r)$, where $\rho_{Li-g}(r)$, $\rho_{Li}(r)$, and $\rho_g(r)$ are the real-space electronic charge distribution of the Li-adsorbed graphene, isolated Li, and free graphene, respectively. By the integral of $\Delta\rho_{cd}(r)$ for the x−y plane, we can get the charge difference $\Delta Q_{cd}(z)$ as a function of the coordinate z. To determine the charge transfer, we need to define a position in the z axis in order to separate the charge of graphene from that of Li. If the position is defined as the half of distance between graphene and Li, $\Delta Q_{cd} \approx 0.27e$ is obtained. If the position is defined as the point at which charge accumulation changes to charge depletion,[30] $\Delta Q_{cd} \approx 0.38e$ is obtained. The different definition of the position results in the different charge transfer can be attributed to the large width of charge distribution along z axis of graphene. For the isolated graphene, the width is about 4 Å. The half of it is larger than the distance between graphene and Li (1.69 Å). The characteristic of the ionic bond is obvious for the interaction of Li and graphene, no matter how the charge transfer is defined.

To identify the effect of defects on the adsorption energy, the DOS of single-vacancy graphene, double-vacancy graphene, single-vacancy graphene with adsorbed Li and double-vacancy graphene with adsorbed Li are calculated (in Figure 7). Because of the introduction of single-vacancy, the local spin is formed and can be attributed to the coupling of one dangle sp^2 orbital and p_z of special carbon on the enneagon around the vacancy.

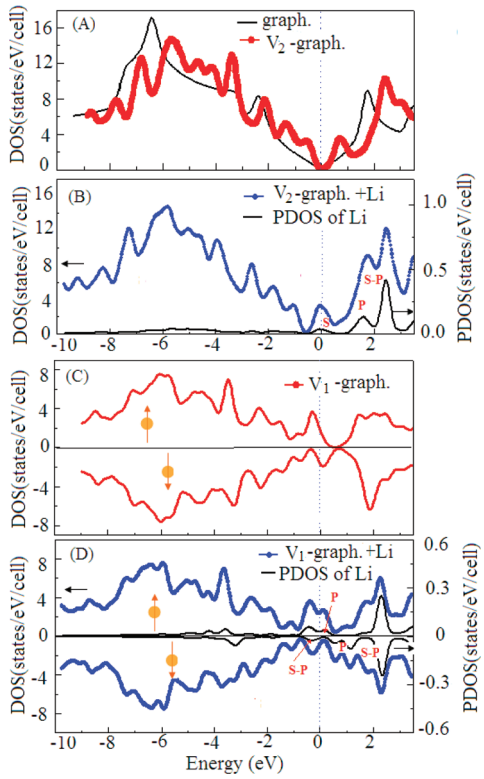

Figure 7. Density of states (DOS) of (A) pristine graphene and graphene with double-vacancy and (C) graphene with single-vacancy, DOS of Li-adsorbed graphene with (B) double-vacancy and (D) single-vacancy. Note that simulation is performed in 4 × 4 unit cell.

The Dirac point is destroyed and two localized spin-polarized bands are formed near Fermi level that results in the nonequivalence of spin-up and spin-down electrons. For the double-vacancy, Fermi level is not shifted and the DOS at Fermi level is zero. However, the DOS near Fermi level is increased, comparing with that of pristine graphene. When Li is adsorbed on the double-vacancy, a charge transferred from Li to graphene results in the upshift of Fermi level. From the PDOS of Li ion, a small part of charge still remains in the 2s orbital of Li. For single-vacancy, it is found that the Fermi level also has a shift. It is possible for a small part of p orbital near Fermi level found in the PDOS of Li to be from that of the carbon p orbital near the Li ion. Because of the increased DOS near Fermi level, the shift of Fermi level is smaller than that of pristine graphene with adsorbed Li.

Due to losing 2s electron, Li ion has a positive charge. From the charge distribution in Figure 8A, the extra charge transferred from Li is mostly around the six carbon atoms near the Li atom, which can be ascribed to the coulomb interaction. Therefore, the hexagonal hole is reduced to prevent the Li ion's entering. For double-vacancy, the electronic density under Li ion is very low, as shown in Figure 8B. The large hole in the charge distribution makes Li ion easily go through the graphene plane with a small diffusion barrier.

4. CONCLUSIONS

The interaction between Li and pristine graphene and that between Li and defective graphene have been studied by first-principles DFT calculations in detail. Considered the Li atom has a trend to form the clusters on graphene with the increase of Li concentration, it is difficult to form Li_2C_2 experimentally,

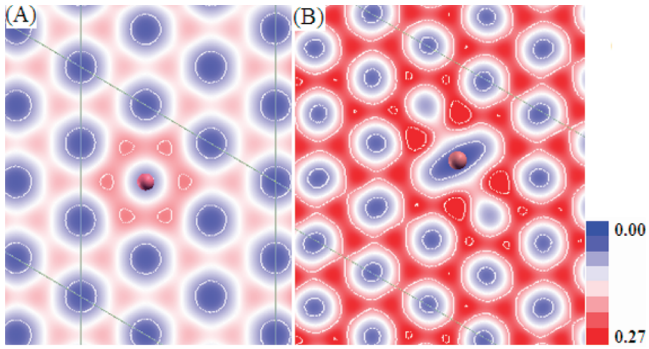

Figure 8. Distribution of charge density in *xy* plane for the region at about 1.25 Å above the graphene plane for (A) Li-adsorbed graphene and (B) at about 0.98 Å above graphene plane for Li-adsorbed graphene with double-vacancy along the *z* direction.

though Li_2C_2 may be a stable structure because of a mixture of sp^2−sp^3. Actually, it is found that the Li/C ratio is less than 1/6 for the single-layer graphene, which is consistent with the results of Raman spectroscopy. Furthermore, it is found that the diffusion of Li ion on graphene is not quicker than that in between two layers of graphite. Therefore, the pristine graphene can not boost the Li/C ratio and diffusion energetics of Li ion, though it can provide two free surfaces.

The defective graphene with single-vacancy and double-vacancy as the models simulate the interaction of Li and carbon of graphene-based nanostructures. It is found that the presence of vacancy defects can enhance the adsorption energy of Li in the region near the defect because of the introduction of extra potential trap. Hence, the graphene-based nanostructures can increase the Li/C ratio significantly. It is also found that Li ion can go through the double-vacancy with a small diffuse barrier. This means that with double-vacancy and higher-order defects, Li ion can diffuse freely go from one side of graphene to other side or the surface of other graphene. The vacancy enhances the diffusion energetics of Li ion to some extent, compared with graphite for which it is difficult for Li ion to diffuse in the direction perpendicular to the graphene sheets. With the analysis of electronic properties and charge distribution, the ionic bonding between Li and C is considered to describe effectively the interaction between Li and carbon in sp^2 carbon system and the charge transfer controls the interaction of Li−carbon nanostructure.

AUTHOR INFORMATION

Corresponding Author

*E-mail: xffan@jlu.edu.cn; wtzheng@jlu.edu.cn.

Notes

The authors declare no competing financial interest.

REFERENCES

(1) Allen, M. J.; Tung, V. C.; Kaner, R. B. *Chem. Rev.* **2009**, *110*, 132−145.
(2) Geim, A. K.; Novoselov, K. S. *Nat. Mater.* **2007**, *6*, 183−191.
(3) Castro Neto, A. H.; Guinea, F.; Peres, N. M. R.; Novoselov, K. S.; Geim, A. K. *Rev. Mod. Phys.* **2009**, *81*, 109.
(4) Geim, A. K. *Science* **2009**, *324*, 1530−1534.
(5) Zhang, Y.; Tan, J. W.; Stormer, H. L.; Kim, P. *Nature* **2005**, *438*, 201−204.
(6) Novoselov, K. S.; Geim, A. K.; Morozov, S. V.; Jiang, D.; Katsnelson, M. I.; Grigorieva, I. V.; Dubonos, S. V.; Firsov, A. A. *Nature* **2005**, *438*, 197−200.
(7) Novoselov, K. S.; Geim, A. K.; Morozov, S. V.; Jiang, D.; Zhang, Y.; Dubonos, S. V.; Grigorieva, I. V.; Firsov, A. A. *Science* **2004**, *306*, 666−669.
(8) Lv, W.; Tang, D.-M.; He, Y.-B.; You, C.-H.; Shi, Z.-Q.; Chen, X.-C.; Chen, C.-M.; Hou, P.-X.; Liu, C.; Yang, Q.-H. *ACS Nano* **2009**, *3*, 3730−3736.
(9) Yoo, E.; Kim, J.; Hosono, E.; Zhou, H.-s.; Kudo, T.; Honma, I. *Nano Lett.* **2008**, *8*, 2277−2282.
(10) Jang, B. Z.; Liu, C.; Neff, D.; Yu, Z.; Wang, M. C.; Xiong, W.; Zhamu, A. *Nano Lett.* **2011**, *11*, 3785−3791.
(11) Kaskhedikar, N. A.; Maier, J. *Adv. Mater.* **2009**, *21*, 2664−2680.
(12) *Lithium Batteries: New Materials, Developments and Perspectives*; Pistoia, G., Ed.; Elsevier: New York, 1994.
(13) Guerard, D.; Herold, A. *Carbon* **1975**, *13*, 337−345.
(14) Dresselhaus, M. S.; Dresselhaus, G. *Adv. Phys.* **1981**, *30*, 139−326.
(15) Kganyago, K. R.; Ngoepe, P. E. *Phys. Rev. B* **2003**, *68*, 205111.
(16) Meunier, V.; Kephart, J.; Roland, C.; Bernholc, J. *Phys. Rev. Lett.* **2002**, *88*, 075506.
(17) Gao, B.; Bower, C.; Lorentzen, J. D.; Fleming, L.; Kleinhammes, A.; Tang, X. P.; et al. *Chem. Phys. Lett.* **2000**, *327*, 69−75.
(18) Tournus, F.; Charlier, J. C. *Phys. Rev. B* **2005**, *71*, 165421.
(19) Liang, M.; Zhi, L. *J. Mater. Chem.* **2009**, *19*, 5871−5878.
(20) Wang, G.; Shen, X.; Yao, J.; Park, J. *Carbon* **2009**, *47*, 2049−2053.
(21) Pan, D.; Wang, S.; Zhao, B.; Wu, M.; Zhang, H.; Wang, Y.; Jiao, Z. *Chem. Mater.* **2009**, *21*, 3136−3142.
(22) Bhardwaj, T.; Antic, A.; Pavan, B.; Barone, V.; Fahlman, B. D. *J. Am. Chem. Soc.* **2010**, *132*, 12556−12558.
(23) Pollak, E.; Geng, B.; Jeon, K.-J.; Lucas, I. T.; Richardson, T. J.; Wang, F.; Kostecki, R. *Nano Lett.* **2010**, *10*, 3386−3388.
(24) Ferre-Vilaplana, A. *J. Phys. Chem. C* **2008**, *112*, 3998−4004.
(25) Martínez, J. I.; Cabria, I.; López, M. J.; Alonso, J. A. *J. Phys. Chem. C* **2008**, *113*, 939−941.
(26) Froudakis, G. E. *Nano Lett.* **2001**, *1*, 531−533.
(27) Zheng, J.; Ren, Z.; Guo, P.; Fang, L.; Fan, J. *Appl. Surf. Sci.* **2011**, *258*, 1651−1655.
(28) Garay-Tapia, A. M.; Romero, A. H.; Barone, V. *J. Chem. Theory Comput.* **2012**, *8*, 1064−1071.
(29) Khantha, M.; Cordero, N. A.; Molina, L. M.; Alonso, J. A.; Girifalco, L. A. *Phys. Rev. B* **2004**, *70*, 125422.
(30) Chan, K. T.; Neaton, J. B.; Cohen, M. L. *Phys. Rev. B* **2008**, *77*, 235430.
(31) Yang, C.-K. *Appl. Phys. Lett.* **2009**, *94*, 163115.
(32) Medeiros, P. V. C.; Mota, F. D.; Mascarenhas, A. J. S.; de Castilho, C. M. C. *Nanotechnology* **2010**, *21*, 115701.
(33) Klintenberg, M.; Lebègue, S.; Katsnelson, M. I.; Eriksson, O. *Phys. Rev. B* **2010**, *81*, 085433.
(34) Dahn, J. R.; Zheng, T.; Liu, Y.; Xue, J. S. *Science* **1995**, *270*, 590−593.
(35) Blochl, P. E. *Phys. Rev. B* **1994**, *50*, 17953.
(36) Hohenberg, P.; Kohn, W. *Phys. Rev.* **1964**, *136*, B864.
(37) Kresse, G.; Furthmüller, J. *Phys. Rev. B* **1996**, *54*, 11169−11186.
(38) Kresse, G.; Furthmüller, J. *Comput. Mater. Sci.* **1996**, *6*, 15−50.
(39) Perdew, J. P.; Chevary, J. A.; Vosko, S. H.; Jackson, K. A.; Pederson, M. R.; Singh, D. J.; Fiolhais, C. *Phys. Rev. B* **1992**, *46*, 6671.
(40) Medeiros, P. V. C.; Mota, F. D.; Mascarenhas, A. J. S.; de Castilho, C. M. C. *Solid State Commun.* **2011**, *151*, 529−531.
(41) Allouche, A.; Krstic, P. S. *Carbon* **2012**, *50*, 510−517.
(42) Chandrakumar, K. R. S.; Ghanty, T. K.; Ghosh, S. K. *Int. J. Quantum Chem.* **2005**, *105*, 166−173.
(43) Krepel, D.; Hod, O. *Surf. Sci.* **2011**, *605*, 1633−1642.
(44) Uthaisar, C.; Barone, V.; Peralta, J. E. *J. Appl. Phys.* **2009**, *106*, 113715−6.
(45) Persson, K.; Sethuraman, V. A.; Hardwick, L. J.; Hinuma, Y.; Meng, Y. S.; van der Ven, A.; Srinivasan, V.; Kostecki, R.; Ceder, G. *J. Phys. Chem. Lett.* **2010**, *1*, 1176−1180.
(46) Toyoura, K.; Koyama, Y.; Kuwabara, A.; Oba, F.; Tanaka, I. *Phys. Rev. B* **2008**, *78*, 214303.

(47) Uthaisar, C.; Barone, V. *Nano Lett.* **2010**, *10*, 2838−2842.
(48) Fan, X.; Liu, L.; Kuo, J.-L.; Shen, Z. *J. Phys. Chem. C* **2010**, *114*, 14939−14945.